OUTPUT OF THE EVAPORATION ENGINE (SLOPING CANOPY)

N.G. Barton

Sunoba Pty Ltd, P.O. Box 1295, Macquarie Centre NSW 2113, Australia

1. Introduction

Thermal technologies for solar power generation include both one-axis concepts (troughs, Compact Linear Fresnel Reflectors) and two-axis concepts (towers, dishes). In general, one-axis concepts collect heat energy at a lower temperature than two-axis concepts. The challenge is to produce electricity as cheaply and reliably as possible, and it is not yet clear which collection temperature or technology will yield the economic optimum, namely the lowest Levelised Electricity Cost (LEC). An alternative third concept is investigated here – power generation from passive solar thermal heat collection. Since the collection temperature will probably be in the range 100-150°C for such a concept, the thermodynamic efficiency will be low, and it will be necessary that both the heat collection process and the heat engine be cheap and simple.

The paper describes new simulations for a heat engine powered by passive solar heat collection under a transparent insulated canopy. Two possibilities for the required 'low ΔT' heat engine would be the Organic Rankine-Cycle and the Stirling Cycle. In addition to their core mechanical components, these engines need heat exchangers to access the sun's energy and condensers or other heat exchangers to dispose of waste heat, and so their specific capital cost ($/kW) is high. Here, an engine with a thermodynamic cycle based on evaporative cooling of hot air at reduced pressure is adopted (Barton, 2008a). This cycle is summarised in Section 2 and can be achieved in a two-stroke piston-in-cylinder engine that is large, multi-cylinder, slow-revving and lightly stressed, without need for heat exchangers or condensers. An experimental version of this engine has been successfully tested (Barton, 2008b) and many other aspects have been studied, including limitations to the engine speed as a result of incomplete evaporation during re-compression.

Recently Barton (2010a) simulated the annual output of the evaporation engine at a suitable site with passive solar heat collection under a horizontal canopy. The site was Wellington in inland New South Wales, Australia: 32.6°S latitude, 148.9°E longitude, 305 m altitude. The present work contains new simulations based on a canopy that slopes at the latitude angle. From knowledge of the total daily incident solar radiation and the sun's position throughout the day, trigonometry gives the direct solar irradiance on the sloping canopy at all times. The instantaneous output of the canopy/engine system was calculated using a heat transfer model of the transparent canopy coupled to the thermodynamic code for the evaporation engine. The air flow-rate under the canopy was chosen to optimise the power output over half-hourly intervals. The power output was aggregated over the day and the whole procedure repeated for a representative sample of days. These aspects are described in Section 3.

In the case of the horizontal canopy, Barton (2010a) showed that the daily power output can be approximated using a linear function of the total daily insolation. For the sloping canopy, however, additional modeling assumptions are required to relate sample results to both the time of year and the total daily insolation. This procedure, which is described in Section 4, enables the daily output to be estimated over the entire year. It is found that the sloping canopy leads to more power output over the year and in a more evenly distributed fashion. The sloping canopy allows a smaller engine than that required for the horizontal canopy. Inclusive of canopy thermal losses but exclusive of engine losses, the annual output from a 1,000 m^2 canopy is estimated as 104 MWhr (horizontal) and 131 MWhr (sloping). Engine losses are expected to reduce these estimates by 25-30%, as described in Section 5.

Passive solar heat collection is relatively cheap and easy, so financial metrics (cost per peak Watt, Levelised Energy Cost) for the canopy/engine system are expected to be favorable, especially for the sloping canopy. These metrics are presented in Section 6. Section 7 concludes the paper with discussion of the developmental pathway for this technology, including current research on heat storage within a bed of loosely packed rocks so as to give despatchable power output when the sun is not shining.

2. Overview of the thermodynamic cycle for the evaporation engine

Figure 1 shows a simulated ideal pressure-volume plot for the piston-in-cylinder evaporation engine. Hot air is taken in through inlet valves, expanded and then spray-cooled at constant volume. Evaporative cooling continues as the air is re-compressed back to atmospheric pressure, whereupon it is released through outlet valves. Air is the heat transfer fluid and the working gas, and the cycle involves *intake – expansion – cooling – compression – exhaust*. This is radically different to usual gas power cycles (*e.g.* Otto, Diesel) based on *intake – compression – heating – expansion – exhaust*. The evaporation engine has natural advantages when air that is already hot or can be heated cheaply is readily available at ambient pressure. The theoretical work output of the cycle is the area inside the *P-V* plot, and is the difference between work expended in expansion and work received in re-compression.

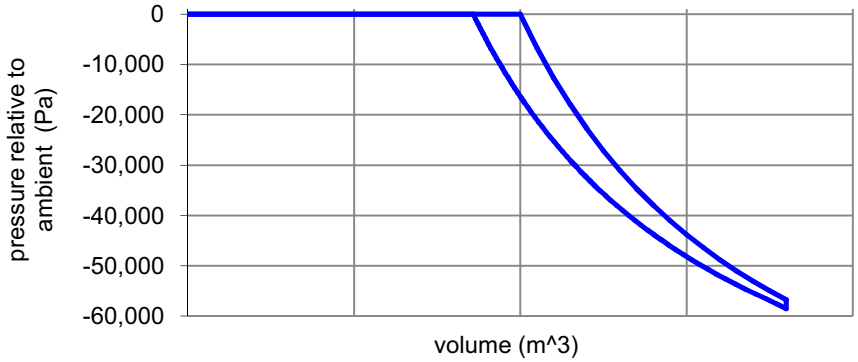

Fig. 1: Pressure-volume plot for the evaporation engine when the inlet temperature is 100°C and the inlet partial pressures are 99.3 kPa for dry air and 2 kPa for water vapour. The ambient temperature (of unheated air and injected water) is 20°C and the expansion ratio is 1.8. For these conditions, the results are: specific work output 7.24 kJ/kg dry air; efficiency 10.8%; specific water consumption 11.8 kg/kWhr. These results do not take account of losses.

Barton (2008a) provides a thermodynamic analysis for the evaporation engine. This assumes that both air and water vapour are ideal gases with constant specific heat capacities. Each stage of the cycle involves coupled algebraic equations for six variables (partial pressure and density of air, partial pressure and density of water vapour, temperature and volume). Expansion takes place along a dry adiabat and is modelled as an isentropic process. Evaporation to saturation at constant volume involves cooling of the air-vapour mixture through uptake of the latent heat of evaporation required to turn liquid water into water vapour. Re-compression of the composite air-vapour-droplet mixture takes place along a moist adiabat, with ongoing evaporation to saturation, and the process requires a numerical solution of the six governing equations. In all cases, the saturation vapour pressure is given by interpolation from tabulated values. The theoretical model assumes that the cycle of the engine is slow enough that there is sufficient time for evaporation to saturation both at constant volume and during re-compression.

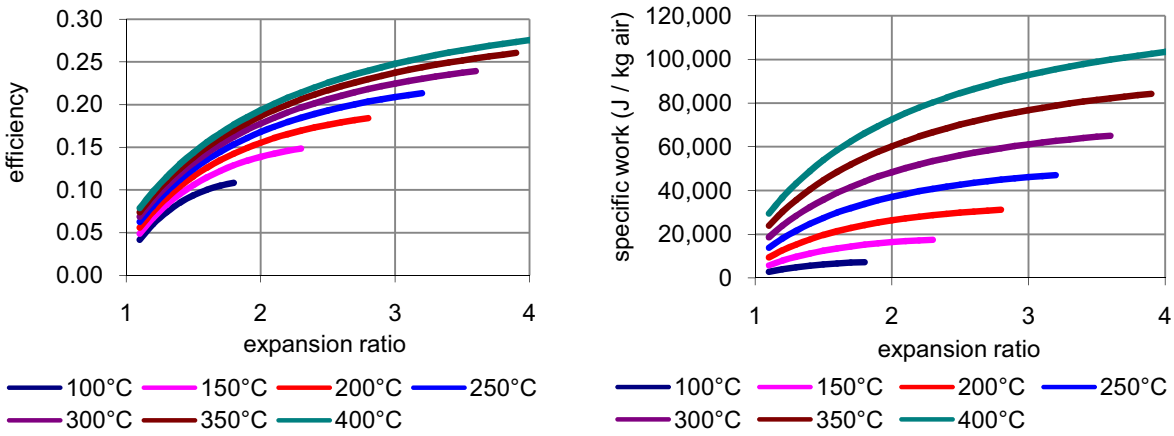

Fig. 2: Theoretical results as a function of inlet temperature and expansion ratio (Barton, 2008a). Left: efficiency; right: specific work/cycle [J/kg air].

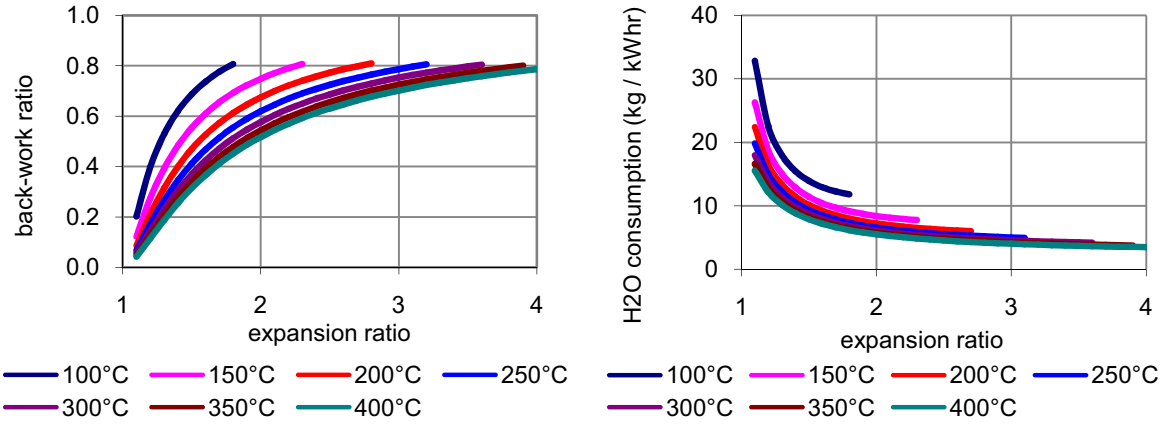

Fig. 3: Theoretical results (Barton, 2008a). Left: back-work ratio; right: specific water consumption [kg/kWhr].

Figures 2 and 3 (Barton, 2008a) show the efficiency, specific work output, back-work ratio and water consumption for various inlet temperatures and expansion ratios when the ambient temperature and water temperature are 20°C and the inlet partial pressures are 99.3 kPa and 2 kPa for air and vapour respectively. The efficiency is the work output divided by the heat energy required to heat ambient air to the inlet temperature at constant pressure. The back-work ratio is the work expended in expansion divided by the work received in re-compression.

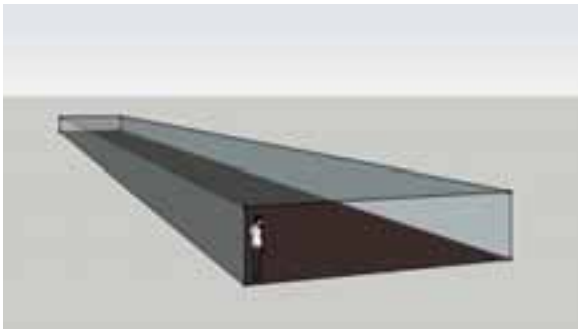

Fig. 4: Illustrating the 1,000 m^2 canopy used in the simulations. The evaporation engine is at one end, but not shown.

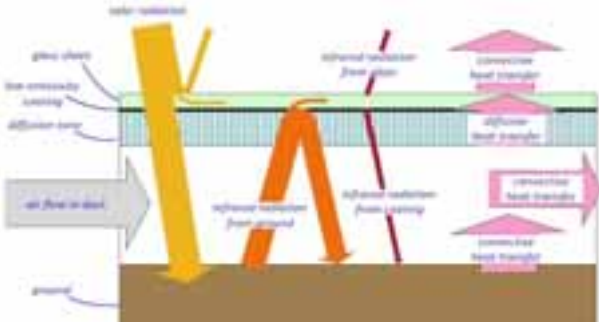

Fig. 5: Elements of the heat transfer model (horizontal canopy).

3. Heat transfer model for the canopy

Figures 4 and 5 show the canopy used in the simulations and the elements of the heat transfer model. Sunlight incident on the canopy is partially reflected, partially absorbed and partially transmitted. A thin layer of ground is warmed by the sun, but otherwise heat transfer into the ground is neglected. Infrared radiation from the ground is substantially reflected by the thin coating on the underside of the glass cover; the remaining infrared radiation from the ground is assumed to be absorbed in the cover. The glass emits infrared radiation from both top and bottom surfaces. There is molecular diffusion of heat through the convection-suppression region (labelled as diffusion zone in Figure 5 and made, for example, from transparent bubbles or slats) and the glass sheet, and convective heat transfer from the outside surface of the glass to the atmosphere. The remaining heat energy is transferred by the airflow to the inlet valves of the evaporation engine.

With the notation given in Appendix A, one-dimensional steady-state heat transfer in the cavity under the glass canopy during any 30-minute period is described by

$$\dot{m}\, C_{aP}\, \frac{dT_a}{dx} = F_s + F_{ir,c2} + F_{ir,g} + F_c \qquad (1)$$

with inlet condition and heat gain/loss terms as follows

$$T_a(0) = T_0 \qquad \text{(inlet condition)} \qquad (2)$$

$$F_s = W\,\tau_{s,c}(\Theta)\,\Phi_s\,\mathbf{n}.\mathbf{s} \qquad \text{(gain; incident solar radiation)} \qquad (3a)$$

$$F_{ir,c2} = W\,\Phi_{ir,c2} \qquad \text{(gain; infrared radiation from cover)} \qquad (3b)$$

$$F_{ir,g} = -W\left(1-\rho_{ir,c2}\right)\Phi_{ir,g} \qquad \text{(loss; infrared radiation from ground)} \qquad (3c)$$

$$F_c = -(W k_a/d)\,(T_a - T_{c2}) \qquad \text{(loss; convection-suppression zone)} \qquad (3d)$$

The ground and air temperatures are assumed identical. In (3a), **n.s** = cos $\boldsymbol{\Theta}$ is given by equation (9) below.

Equation (1) involves the temperature at the underside of the glass cover and must therefore be solved jointly with an equation for heat transfer in the cover, namely

$$\frac{d^2T_c}{dz^2} = -\frac{1}{ek_c}\left\{\alpha_{s,c}\,\Phi_s\,\cos\Theta + \alpha_{ir,c}\,\Phi_{ir,g}\right\} \qquad (4)$$

subject to boundary conditions

$$-\left[k_c\frac{\partial T_c}{\partial z}\right]_{z=H} = \frac{k_a}{d}\,(T_a - T_{c2}) - \Phi_{ir,c2} \qquad \text{(bottom surface)} \qquad (5a)$$

$$-\left[k_c\frac{\partial T_c}{\partial z}\right]_{z=H+e} = h_{c/o}\,(T_{c1} - T_o) + \Phi_{ir,c1} \qquad \text{(top surface)} \qquad (5b)$$

In (4), absorption of sunlight and infrared radiation is averaged across the thickness, *e*, of the glass cover. The boundary condition (5a) at the bottom surface of the glass cover involves competing effects due to heating (by molecular diffusion through the convection-suppression region) and cooling (by infrared radiation). At the top surface (5b), there is cooling due to convective heat transfer and radiation. All radiation terms in the above equations take the general form

$$\Phi = \varepsilon\sigma T^4 \qquad (6)$$

in which the emittance ε and absolute temperature *T* are appropriate to the emitting surface.

Data

The Bureau of Meteorology routinely provides minimum and maximum daily temperatures for observation stations, as well as temperature and relative humidity at 0900 and 1500 hours. The ambient temperature throughout the day, T_0, was modelled by a quadratic-cubic spline approximation to the data, in which the minimum and maximum were assumed to be at 0500 and 1230 hours (with adjustment for daylight saving time as appropriate). The vapour partial pressure throughout the day was taken to be the average of the readings for 0900 and 1500 hours. Wellington is 305 m above sea level, and the atmospheric pressure was taken as 97,630 Pa throughout the year.

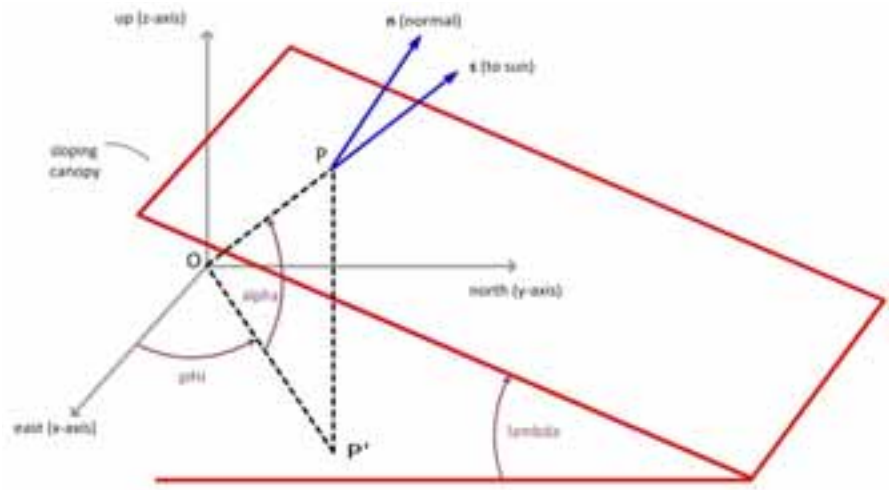

Fig. 6: Illustrating the unit vectors n and s.

The solar radiation impinging on the canopy is now calculated (based on a southern hemisphere location). As illustrated in Figure 6, let (x,y,z) be Cartesian coordinates, with x to the east, y to the north and z vertical. The canopy is indicated by red lines and slopes to the north at an angle λ to the horizontal. Let P be a point on the canopy such that OP points towards the sun; P' is the projection of P on the (x,y) plane. The altitude α is the angle between OP and the (x,y) plane. The angle φ is the angle between OP' and the x-axis. The unit vector **n** is normal to the plane of the canopy and the unit vector **s** points towards the sun.

It follows that

$$\mathbf{n} = (0, \sin\lambda, \cos\lambda) \qquad \text{and} \qquad \mathbf{s} = (\cos\alpha\cos\varphi, \cos\alpha\sin\varphi, \sin\alpha) \tag{7,8}$$

If Φ_s is the radiant flux intensity due to sunlight, then the component of solar radiation hitting the canopy is

$$\Phi_s\,\mathbf{n}.\mathbf{s} \;=\; \Phi_s\,(\sin\lambda\cos\alpha\sin\varphi + \cos\lambda\sin\alpha) \tag{9}$$

The angles α and φ were obtained at 15-minute intervals from www.sunposition.info (in fact for Mudgee, about 50 km to the east of Wellington). The radiant solar flux intensity averaged over the day, Φ_s, was obtained by considering the integral

$$\int_{\text{sunrise}}^{\text{sunset}} \Phi_s \sin\alpha(t)\; dt \;=\; \Phi_s \,.\, \int_{\text{sunrise}}^{\text{sunset}} \sin\alpha(t)\; dt \tag{10}$$

which leads to the total insolation on a horizontal surface in MJ.$(m^2.day)^{-1}$, as provided by the Bureau of Meteorology. Variations in Φ_s due to air mass and diffuse radiation were not included in the model. About 5% of the insolation data were not available, presumably due to equipment failure. Missing values were filled in using estimates based on hours of sunshine and temperature data for the days in question. The canopy was either horizontal or sloping at the latitude angle, $\lambda = 32.6°$.

The reflectance ρ and transmittance τ for the glass sheet were taken to be those for low-emissivity glass manufactured by Pilkington (2005). The absorptance α was given by $\alpha = 1 - (\rho + \tau)$. Coefficients for sunlight were taken as the average of Pilkington data for 350-2,500 nm wavelength and coefficients for infrared radiation as the average for 3,000-20,000 nm wavelength. A correction due to Mitalas & Stephenson (1962) was applied to give the effect of the angle of incidence on the transmission and reflection coefficients, with the absorption coefficient held constant. This gives the incidence angle modifier (IAM) for coefficients. For calculations of emitted infrared radiation, the emittance ε was taken to be the same as the absorptance α. As in Barton (2008a), the heat transfer model assumed both air and water vapour were ideal gases with constant specific heat capacities. The gas properties and other parameters are as described in Appendix B.

Numerical procedures

The following procedures were used to simulate the output of the canopy-engine system on any given day. The averaged direct solar irradiance Φ_s was calculated using equation (10) and the ambient temperature smoothly approximated by a cubic-quadratic spline. For any 30-minute interval, the incident solar radiation was given by Φ_s **n.s**. The effect of water vapour was neglected for heating under the canopy, but necessarily was included for the calculation of the thermodynamic cycle in the evaporation engine.

Equations (1-5) were solved by a predictor-corrector method. For the predictor step, temperature and radiation values were approximated by those at the previous spatial location. A forward-Euler method was used to give an approximation to the temperature at the new spatial location. The predicted temperature values were then used to obtain the solution to equation (4), which always takes the form $T_c = s_0 + s_1 z + \zeta z^2/2$, in which ζ is the right-hand side of (4) and the constants s_0 and s_1 are determined from the boundary conditions (5a,b). That allows terms (3a-d) to be approximated at the new spatial location, thereby enabling a corrector step with an improved approximation to the solution.

Once the outlet air temperature was known, the previously developed thermodynamic code (Barton, 2008a) was used to predict the power output of the engine and other operating parameters. The key factor controlling the performance of the canopy-engine system is the mass flow-rate of air, $\dot{m}$, which is expressed in (kg air) s^{-1}. As $\dot{m}$ becomes larger, the temperature attained under the canopy and the specific work output

(J (kg air)$^{-1}$) of the evaporation engine become less. However, canopy losses (infrared radiation and heat transfer from the top surface) are also reduced, and since $\dot{m}$ is larger that acts to increase the power output of the engine. A simple root-finding procedure was used to find the optimal flow-rate $\dot{m}$. In a few cases with cool ambient conditions and low insolation levels, especially early morning and late afternoon, $\dot{m}$ was also limited by assuming that the air in the engine was always above freezing after expansion by the factor r.

Tests confirmed that suitable accuracy could be obtained with 50 spatial steps. The overall heat budget for the canopy was routinely checked and always accurate to better than 1%. Losses from the top surface included reflection of sunlight, emission of infrared radiation and convective heat transfer.

4. Results

To generate a sample of results, the output of the canopy-engine system was calculated on the 15th day of each month from March 2009 to February 2010. For each 30-minute period, the flow-rate was chosen to optimise the power output. Illustrative results are first shown for 15 September 2009 (spring conditions) and 15 December 2010 (summer conditions). All 12 monthly results were then jointly analysed to develop procedures to predict the annual output.

Results for 15 September 2009 are shown in Figures 7a-c. This was a fine and sunny spring day, with maximum temperature 24.9°C, 8.5 hours sunshine, 21.03 MJ m^{-2} insolation on a horizontal surface, and relative humidity of 74% and 38% at 0900 and 1500 hours respectively. All results are for a canopy with glass area 1,000 m^2. The sloping canopy receives more sunshine at all times of the day than a horizontal canopy. As a result, the theoretical power output of the sloping canopy is 45% more than for the horizontal canopy over the course of the day. Figures 8a-c show corresponding results for 15 January 2010. This was a warm to hot summer's day, with maximum temperature 33.5°C, 8.5 hours sunshine, 30.49 MJ m^{-2} insolation on a horizontal surface, and relative humidity of 63% and 41% at 0900 and 1500 hours respectively. Again, results are for a canopy with glass area 1,000 m^2. Under the summer conditions, the sloping canopy now receives less sunshine at all times of the day than a horizontal canopy. As a result, the theoretical power output of the sloping canopy is 18% less than for the horizontal canopy over the course of the day.

For the 12 days that were explicitly simulated, the aggregated daily power output in kWhr (including canopy losses but not engine losses) is shown in Figure 9 as a function of total daily insolation on a horizontal surface. Results are shown for both horizontal and sloping canopies on the same days. For the horizontal canopy (red squares), it is reasonable to model the daily power output as a linear function of daily insolation. That was the approach taken by Barton (2010a), with the result

$$y = 23.13\,x - 187.5 \qquad (11)$$

where the output y is in kWhr (1,000 m^2)$^{-1}$ day^{-1} and the insolation x is in MJ m^{-2} day^{-1}. The situation is different however for the sloping canopy (blue circles); a linear approximation is evidently unsuitable, as would be simple quadratic or cubic approximations.

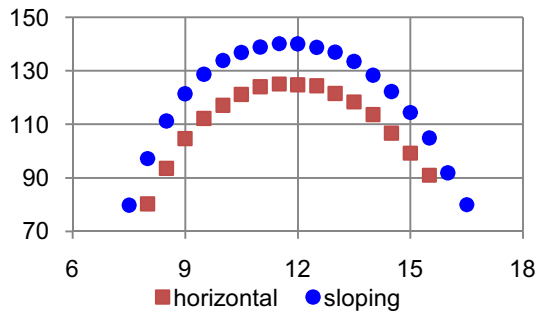

Fig. 7a: Optimal outlet temperature (°C) at half-hour intervals on 15 September 2009.

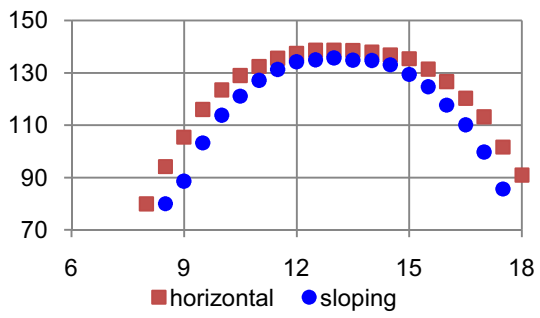

Fig. 8a: Optimal outlet temperature (°C) at half-hour intervals on 15 January 2010.

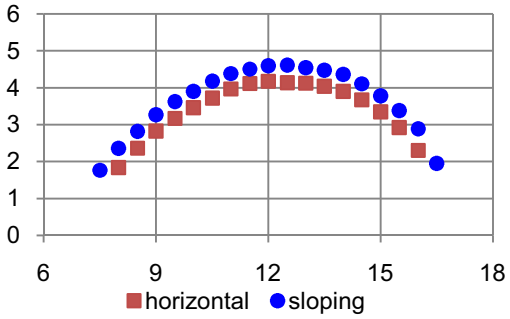

Fig. 7b: Optimal air flow-rate (kg s^{-1}) at half-hour intervals on 15 September 2009.

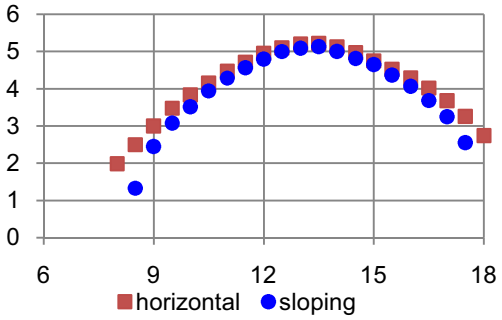

Fig. 8b: Optimal air flow-rate (kg s^{-1}) at half-hour intervals on 15 January 2010.

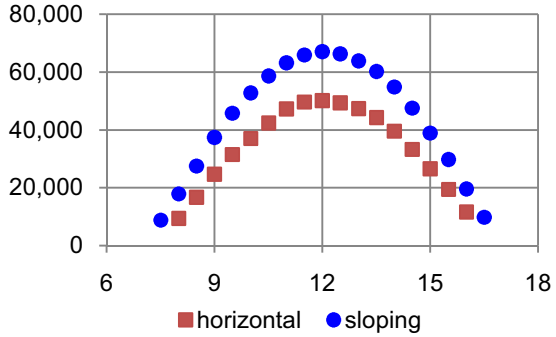

Fig. 7c: Optimal power output (W) at half-hour intervals on 15 September 2009.

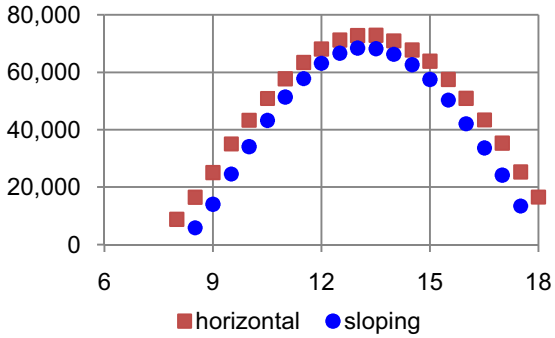

Fig. 8c: Optimal power output (W) at half-hour intervals on 15 January 2010.

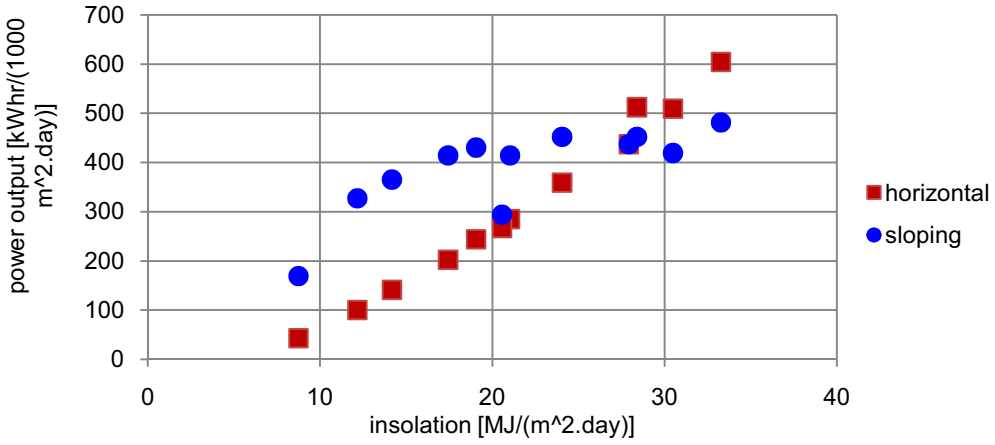

Figure 9: Daily power output in kWhr (1000 m^2)$^{-1}$ day^{-1} as a function of insolation on a horizontal surface in MJ m^{-2} day^{-1}.

A general observation from the calculations and Figure 9 is that the daily power output is greater for the sloping canopy than for the horizontal canopy during winter (significantly so), spring and autumn. The output is less in summer however. That general conclusion is supported by Figures 7 and 8 above and follows logically from the amount of direct solar radiation intercepted by the sloping canopy compared to the horizontal canopy. The situation is made more complicated, however, because some of the low-insolation daily results in Figure 9 are for cloudy spring or autumn days, and not from winter days. The sloping canopy results need to be approximated using a model that takes into account both the time of the year and the cloudiness of the day in question. This model is now developed.

Figure 10 shows the observed daily insolation (MJ m^{-2}) on a horizontal surface at Wellington for 365 days starting from 1 March 2010. Also shown on Figure 10 is the expression

$$f(n) = 24.1 - 10.85 \sin \{2\pi(n\text{-}22)/365\} \qquad (12)$$

which approximates the optimal (cloud-free) insolation that could be expected on day n of the year. At day 22 (corresponding to the autumn equinox, 22 March), the insolation takes the mean value 24.1 MJ m^{-2}. For other days the optimal insolation varies sinusoidally as a function of n with amplitude 10.85 MJ m^{-2} and period 365 days. Note that while (4) appears to be a reasonable description of the insolation received, no attempt is made to give the formula a theoretical justification.

The maximum power output that could be received for any particular level of insolation, under perfect weather conditions, can now be modelled by the quadratic function

$$p(x) = c_1 x (1 + c_2 x) \qquad (13)$$

where x in MJ m^{-2} day^{-1} represents the insolation received on a horizontal surface during a day. This expression is shown by the solid line in Figure 11. The power output is in kWhr $(1{,}000\ m^2)^{-1}$ day^{-1}, and the numerical values of the constants are $c_1 = 34.5$ and $c_2 = -0.01725$. It is noted that (13) has been used as a reasonable representation for the optimal envelope, without theoretical justification.

Now let $g(n)$ be the observed insolation in MJ m^{-2} day^{-1} received on day n of the year. The power output $q(n)$ in kWhr $(1{,}000\ m^2)^{-1}$ day^{-1} on given day n is approximated by

$$q(n) = p(f(n)) \left\{ 1 - \gamma \left[\frac{f(n) - g(n)}{f(n)} \right] \right\} \qquad (14)$$

where the coefficient γ is chosen to give the least-squares best fit between $q(n)$ and the calculated power output for the sample of 12 days that were simulated in detail. That process gives $\gamma = 1.34$. As with (12) and (13), equation (14) has been used merely for descriptive purposes, without theoretical justification. To interpret approximation (14) in words, the simulated power output is the perfect power output given perfect insolation for the day in question, reduced by a multiplicative factor which is linear in the relative shortfall in the amount of insolation compared to the perfect amount of insolation.

The outcome is shown in Figure 11, in which the pink squares show approximation (14) for the 12 days that were simulated. The most significant discrepancy between the blue circles and pink squares occurs for x = 28.40 MJ m^{-2}, which corresponds to 15 November 2009. This day was unusual in that it was not especially sunny (hence the received insolation was clearly less than perfect) but it was hot (38°C maximum, 36.9°C at 1500 hours), which meant that heat losses from the canopy were reduced and the power output was higher than might have otherwise been expected. As Figure 9 shows, the power output from the horizontal canopy was also above the theoretical prediction on this day.

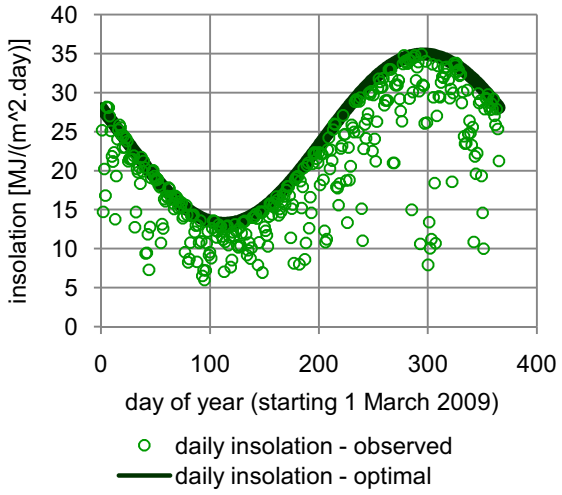

Fig. 10: Observed and approximate optimal insolation on a horizontal surface in MJ $m^{-2}day^{-1}$ for 365 days starting from 1 March 2010.

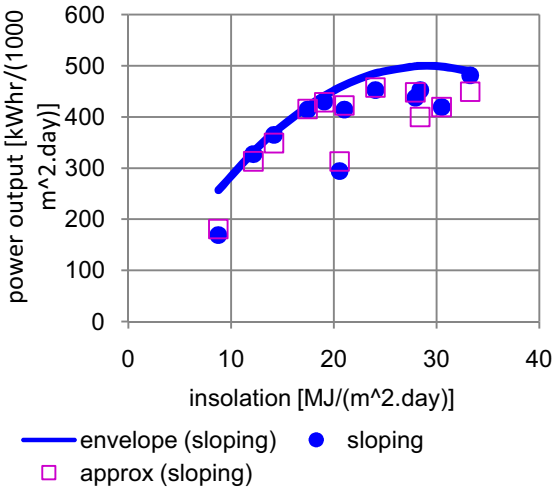

Fig. 11: Results for the sloping canopy. Blue circles show the calculated power output for the 15th day of each month from March 2009 to February 2010. Pink squares show approximation (14) for these 12 days. The solid line is the envelope for daily power output given perfect weather conditions at any given level of insolation.

Based on the above procedures for sloping canopies, Figure 12 displays the simulated power output for every day of the year. Monthly averages are also shown, as are results for horizontal canopies. Note that these results are for a canopy-engine system in which the glass area of the canopy is 1,000 m^2. Canopy losses are included, but not engine losses. It is immediately clear that the daily power output is more uniform throughout the year for the sloping canopy than for the horizontal canopy. The maximum daily power output of the horizontal canopy system clearly occurs in summer, whereas for the sloping canopy system there is not much difference in the daily power output between summer, autumn and spring. For the sloping canopy-engine system, the annual power output is estimated to be 131 MWhr $(1{,}000\ m^2)^{-1}$ $year^{-1}$, some 26% higher than for the horizontal canopy-engine system.

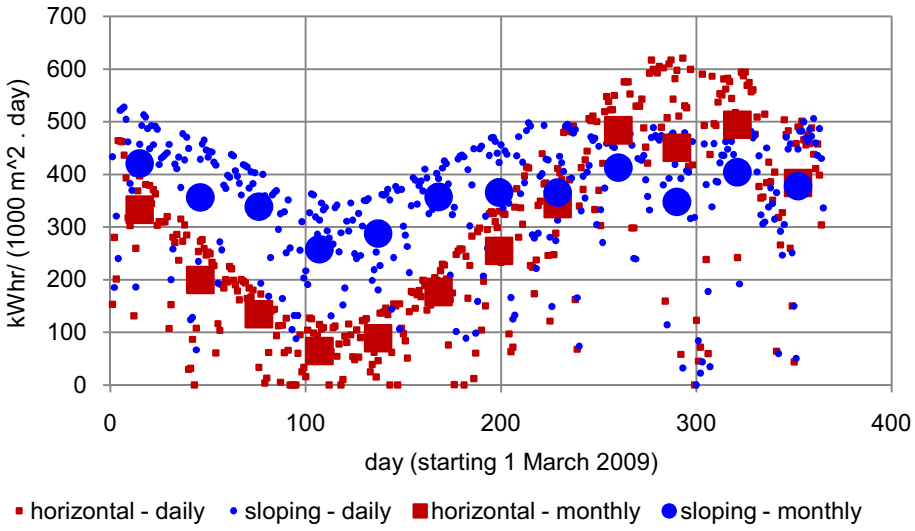

Fig. 12: The simulated power output for every day of the year for both horizontal and sloping canopies. Monthly averages are also shown.

The water consumption for the sloping canopy system is plotted in Figure 13. Also shown is the linear approximation $w = 9.258\ q + 112.1$, where q has units kWhr $(1{,}000\ m^2)^{-1}$ day^{-1} and w has units litres $(1000\ m^2)^{-1}$ day^{-1}. Using this linear approximation and the approximation (14), the total simulated water consumption for the sloping 1,000 m^2 canopy-engine system over the entire year is estimated to be 1,250 m^3 $(1{,}000\ m^2)^{-1}$ $year^{-1}$, which is approximately 20% greater than for the horizontal canopy-engine system.

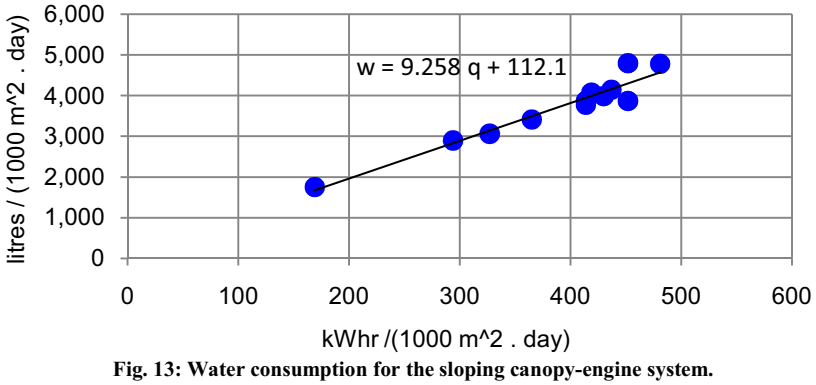

Fig. 13: Water consumption for the sloping canopy-engine system.

5. Losses

The calculations presented so far are an over-estimate in that they include canopy losses but not engine losses. Engine losses for the sloping canopy-engine system are now estimated. Table 1 below is reprinted without modification from Barton (2010a), whilst Table 2 contains fresh calculations specific to the sloping canopy-engine system. To minimise incomplete evaporation during re-compression, the amount of water to be purified and injected is taken to be 125% of the theoretically predicted amount (Barton, 2010b). As in the

case of the horizontal canopy (Barton, 2010a), expected engine losses amount to 25-30% of the theoretical power output after canopy losses, leaving 70-75% of the theoretical output as the actual output.

Table 1: Engine losses.

	% loss	Comments
Category A. Losses that reduce the available heat energy		
Transient heat transfer	7	This estimate is uncertain; the loss is reduced as the engine becomes bigger and faster revving.
Leakage around valves and seals	1	Not expected to be significant.
Dead zones	1	Not expected to be significant.
Category B. Losses affecting the engine operation		
Incomplete evaporation during re-compression	4	This is the major limitation on the engine speed, and has been extensively studied elsewhere (Barton, 2010b). Satisfactory performance is obtained if 25% more water than theoretically predicted is injected and the engine runs at 1 Hz.
Aerodynamic losses in valves	1	Not expected to be significant since the engine will have generous valves and be slow-revving.
Mechanical friction	4	A standard engineering challenge.
Category C. Water losses		
Water purification		The energy requirement for a reverse osmosis system is approximately 15 kJ kg^{-1} or 0.004 MWhr m^{-3}. See Table 2.
Water injection		The water pump pressure is 10 MPa and the energy requirement is 10 kJ kg^{-1} or 0.0028 MWhr m^{-3}. See Table 2.
Category D. Electrical losses		
Mechanical to electrical conversion	3	A standard engineering challenge.

Table 2: Annual power output for the sloping 1,000 m^2 system after engine losses.

Predicted output with no engine losses	131 MWhr
Mechanical output after 18% losses in Categories A and B	131 × 0.82 = 107 MWhr
Energy requirement for water purification (Category C)	1,250 m^3 ×0.91×1.25× 0.004 MWhr m^{-3} = 5.7 MWhr
Energy requirement for water injection (Category C)	1,250 m^3 ×0.91×1.25× 0.0028 MWhr m^{-3} = 4.0 MWhr
Energy loss in mechanical to electrical conversion (Category D)	107 × 0.03 = 3.2 MWhr
Estimated power output	107 – (5.7+4.0+3.2) = 94 MWhr

Table 3: Financial metrics for a 1,000 m^2 sloping canopy-engine system. The peak power output is 60 kW after all canopy and engine losses.

Cost of land, earthworks, frame and glass	25m^{-2}$, so $25,000 per canopy
Cost of engine and balance of plant	$1,000 $(kW)^{-1}$, so $60,000 for a 60 kW engine
Capital cost	$85,000
Interest rate	8%
Rate of capital return (based on 8% interest and 20 year pay-back)	10.2%
Capital expenditure per year	0.102 yr^{-1} ×$85,000 = $8,670 yr^{-1}
Operating expenditure per year	4% of capital cost, so $3,400 yr^{-1}
Expenditure per year	$12,070 yr^{-1}
Metric 1: cost per peak Watt	$85,000/60,000W = $1.42 $(W_p)^{-1}$
Metric 2: levelised electricity cost	$12,070/94 MWhr = $128 $(MWhr)^{-1}$

6. Financial metrics

For the sloping canopy-engine system, the maximum theoretical instantaneous power output over the 12 days that were carefully simulated was 77 kW. Perhaps slightly higher output might be obtained for particularly hot and sunny days not simulated during the year. After allowing for 25-30% inevitable engine losses, it is therefore reasonable to assume that a 60 kW engine would be appropriate for the 1,000 m^2 sloping canopy. (The corresponding figure for the horizontal canopy was 65 kW.) This enables financial metrics to be prepared (Table 3). These calculations include estimates for all canopy and engine losses. The metrics depend on financial, manufacturing and operational assumptions that, at this stage, must be regarded as preliminary. Taxation issues are not included in the calculations.

7. Conclusion

Table 4 summarises the key results of this study of the canopy-engine system in which the canopy slopes at the latitude angle. The site for the simulations is Wellington in inland New South Wales, latitude 32.6°, and the work is based on the period from March 2009 to February 2010. Results for a horizontal canopy (Barton, 2010a) are also shown in Table 4. In comparison to the horizontal system, the sloping system gives 27% more annual power output, which is more evenly distributed over the year and is obtained with a slightly smaller engine. The cost per peak Watt is 3% higher for the sloping system. The levelised electricity cost is 35% lower for the sloping system.

Table 4: Summary of results for the passive solar canopy-engine system. Results are for a 1,000 m^2 canopy and are inclusive of all losses. The output is electrical power.

	Units	Horizontal	Sloping
Peak power	kW	65	60
Annual output	MWhr yr^{-1}	74	94
Annual water consumption	m^3 yr^{-1}	1,181	1,422
Financial metric 1	AUD $(W_p)^{-1}$	1.38	1.42
Financial metric 2	AUD $(MWhr)^{-1}$	173	128

Current work with this concept focusses on heat storage in a bed of loosely packed rock fragments. It is anticipated that this will enable power generation at constant levels and when the sun is not shining. It is intended that simulation results will be presented to the Australian Solar Energy Society Conference in late 2011. Another important issue is the mechanical principle for the piston-in-cylinder evaporation engine. Barton (2008b) reported serious shortcomings with the mechanical principle for his experimental evaporation engine. A greatly-improved mechanical concept has been developed, although this needs further development and remains an industrial secret at present.

8. References

Barton, N.G., 2008a. An evaporation heat engine and condensation heat pump, *ANZIAM J.* 49, 503-524.

Barton, N.G., 2008b. Experimental results for a heat engine powered by evaporative cooling of hot air at reduced pressure, in *Proc Australian and New Zealand Solar Energy Society Conference*, Sydney.

Barton, N.G., 2010a. Annual output of a new solar heat engine, in *Proc Australian Solar Energy Society Conference*, Canberra.

Barton, N.G., 2010b. Simulation of incomplete evaporation for BEE re-compression; T_{inlet} = 200°C, *Technical Report 2010-1*, Sunoba Pty Ltd.

Mitalas, G.P., Stephenson, D.G., 1962. Absorption and transmission of thermal radiation by single and double glazed windows, *Div Building Research, National Research Council of Canada*, 173.

Pilkington Technical Information ATS-138 (2005).

Appendix A: Notation

C	specific heat capacity	[J kg^{-1} K^{-1}]
d	thickness of the convection-suppression zone	[m]
e	thickness of glass cover	[m]
F	terms used in equation (1)	[W m^{-1}]
$h_{c/o}$	convective heat transfer coefficient	[W m^{-2} K^{-1}]
k	thermal conductivity	[W m^{-1}K^{-1}]
$L,H.W$	length, height, width of the canopy	[m]
$\dot{m}$	mass flow rate of air under canopy	[kg s^{-1}]
n	unit normal to canopy	[-]
r	expansion ratio of the evaporation engine	[-]
s_0,s_1	coefficients in solution of equation (2)	[K,K m^{-1}]
s	unit normal towards sun	[-]
t	time throughout the day	[s]
T	temperature	[K]
x,z	lengthwise, normal coordinates relative to canopy	[m]
x,y,z	east, north, vertical coordinates in Fig. 6.	[m]
$\alpha,\varepsilon,\rho,\tau$	absorptance, emittance, reflectance, transmittance	[-]
α	sun angle (altitude)	[radian]
δx	element of length lengthwise in the duct	[m]
ζ	right-hand side of equation (4)	[K m^{-2}]
η	canopy efficiency	[%]
$\boldsymbol{\Theta}$	angle of incidence of sunlight on canopy	[radian]
ρ	density	[kg m^{-3}]
σ	Stefan-Boltzmann coefficient	[W m^{-2} K^{-4}]
Φ	radiant flux density	[W m^{-2}]

Subscripts

a	air
c	cover (glass), c_1 outside surface, c_2 inside surface
c/o	cover to ambient
g	ground
ir	pertaining to infrared radiation from ground and cover, 3000 – 20000 nm
o	ambient
P,V	constant pressure, constant volume
s	sun, pertaining to solar radiation, 350 – 2,500 nm
v	water vapour

Appendix B: Parameter values for the simulations.

(* Mitalas-Stephenson correction not applied here.)

L	100 m	$\alpha_{s,c}$	0.18	C_{aP}	1,005 J kg^{-1} K^{-1}
W	10 m	$\rho_{s,c}$	0.12 *	C_{aV}	718 J kg^{-1} K^{-1}
H	2 m	$\alpha_{ir,c}$	0.15	C_{vP}	1,872 J kg^{-1} K^{-1}
d	0.025 m	$\rho_{ir,c}$	0.85	C_{vV}	1,411 J kg^{-1} K^{-1}
e	0.003 m	ρ_c	2,500 kg m^{-3}	k_a	0.0261 W m^{-1}K^{-1}
δx	2 m	k_c	1.20 W m^{-1} K^{-1}	$h_{c/o}$	50 W m^{-2} K^{-1}
r	1.9	C_c	840 J kg^{-1} K^{-1}	σ	5.67×10^{-8} W m^{-2} K^{-4}